Physica D 241 (2012) 1406–1416

Contents lists available at SciVerse ScienceDirect

Physica D

journal homepage: www.elsevier.com/locate/physd

On stability of generalized short-crested water waves

Travis McBride, David P. Nicholls *

Department of Mathematics, Statistics, and Computer Science, University of Illinois at Chicago, Chicago, IL 60607, United States

ARTICLE INFO

Article history:
Received 5 January 2012
Received in revised form
17 February 2012
Accepted 11 May 2012
Available online 26 May 2012
Communicated by J. Bronski

Keywords:
Stability
Two-dimensional periodic traveling water waves
Generalized short-crested Waves
Boundary perturbation methods

ABSTRACT

In this paper, we take up the question of dynamic stability of genuinely two-dimensional "generalized" hexagonal traveling wave patterns on the surface of a three-dimensional ideal fluid (i.e., stability of Generalized Short-Crested Wave (GSCW) solutions of the water wave problem). We restrict ourselves to a study of spectral stability which considers the linearization of the water wave operator about one of these traveling generalized hexagonal waves, and draws conclusions about stability from the spectral data of the resulting linear operator. Within the class of perturbations we are allowed to study, for a wide range of geometrical parameters, we find stable traveling waveforms which eventually destabilize with features that depend strongly on the problem configuration. In particular, we find "Zones of Instability" for patterns shaped as symmetric diamonds, while such zones are absent for asymmetric configurations. Furthermore, we note that within a geometrical configuration, as a "generalized SCW" ratio is varied (essentially the character of the linear solution), these waves become more unstable as the waves become more asymmetric.

1. Introduction

The movement of a large body of water under the influence of gravity (e.g., the ocean) is governed by the Euler equations of ideal fluid mechanics (the water wave problem), and arises in a wide array of engineering applications. From pollutant transport to the motion of sandbars to tsunami propagation, the water wave equations are a central model in fluid mechanics. Among the many motions permitted by these equations, the periodic traveling wave solutions are of great interest due to their ability to transport energy and momentum over great distances in the ocean. Of course not all of these traveling waveforms are dynamically stable and it is of crucial importance to identify those that are.

A great deal of research has been conducted on the stability of two-dimensional (one vertical and one horizontal) periodic wavetrains, the so-called "Stokes waves". The striking result of Benjamin and Feir [1] that such waves on deep water are dynamically *unstable* set off a decades-long investigation into the strength and timescales of such instabilities as functions of the allowed properties of potential perturbations (e.g. superharmonic [2], subharmonic [3], and three-dimensional [4–7]). The interested reader is referred to the excellent survey article of Dias and Kharif for a complete review [8].

In this paper, we take up the question of dynamic stability of genuinely two-dimensional "generalized hexagonal" traveling wave patterns on the surface of a three-dimensional fluid. Such waves (which we denote "Generalized Short-Crested Waves"—GSCWs) have traveling surface shapes $\eta(x)$ with leading order behavior

$$\eta_1(x) = \rho_1 \cos(k_1 \cdot x) + \rho_2 \cos(k_2 \cdot x),$$

for linearly independent wavenumbers k_1 and k_2. By contrast, Stokes waves feature a single wavenumber ($\rho_1 = 0$ or $\rho_2 = 0$), while classical "Short-Crested Waves" (SCWs) require that $\rho_1 = \rho_2$ so that η_1 resembles a diamond and η becomes "rectangular" as it becomes more nonlinear [9,10].

SCWs have been the subject of a good deal of recent work which begins with the high-order numerical simulations of Roberts [11], and Roberts and Peregrine [12] (see also the work of Marchant and Roberts [13] in finite depth). One of the authors has contributed to their study, first (in collaboration with W. Craig) through a rigorous theoretical analysis of their existence [14] and supplementary numerics [9,10]. Later, in collaboration with F. Reitich, he developed a stable and high-order numerical algorithm for their computation [15] which also delivers a powerful and straightforward rigorous existence theory [16].

Regarding the stability of these SCWs, current results are restricted "spectral stability" which considers the linearization of the water wave operator about one of these traveling rectangular waves, and draws conclusions about stability from the spectral data of the resulting linear operator. Along these lines the definitive work is the numerical simulations of Ioualalen and Kharif for superharmonic [17] and subharmonic [18–20] perturbations. We also mention the extensive finite-depth work of Ioualalen, Kharif, and collaborators [21–24]. In short, these

* Corresponding author. Tel.: +1 312 413 1641; fax: +1 312 996 1491.
E-mail address: nicholls@math.uic.edu (D.P. Nicholls).

0167-2789/$ – see front matter © 2012 Elsevier B.V. All rights reserved.
doi:10.1016/j.physd.2012.05.009

authors focused their attention on resonant configurations of wavenumbers in the basic traveling wave (i.e., k_1 and k_2) with wavenumbers in the leading perturbation. These linear resonances govern the instability of these nonlinear traveling waveforms for *sufficiently small* amplitudes, while nonlinear effects dictate which perturbations are strongest. However, as the amplitude is increased other mechanisms for instability enter and move the strongest instabilities to other points, sometimes far from the linear resonance curves.

In this paper, we investigate the role of asymmetry in the stability theory of SCWs both with regard to their geometric configuration (through their underlying period) and their linear character (through the ratio ρ_1/ρ_2). While we are able to draw some conclusions regarding this question, we do point out that we are not able to accommodate *all* possible unstable perturbations due to computational limitations. Consequently, the conclusions we draw regarding *instability* can be viewed as authoritative, however, conclusions regarding *stability* may not be conclusive as we possibly may have excluded an unstable perturbation form (see Section 2.5 for more details). For the question of geometric asymmetry, we note that as the waveforms are varied away from the symmetric case ($\theta = 45^\circ$, symmetric diamond-shaped), waves of similar height become more unstable. Perhaps more surprisingly, we noticed a "Zone of Instability" in the symmetric case – a band of wave heights which are unstable with stable waveforms of smaller *and* larger height – which does *not* exist in the asymmetric cases. In these, instability sets in for a certain value of the wave height and then all taller waves are also unstable. Regarding the linear character, we found a *destabilizing* effect with the decrease of the ratio ρ_1/ρ_2 where the initial onset of instability occurs for smaller values of the wave height for smaller choices of this ratio.

The paper is organized as follows. In Section 2, we recall the equations of motion together with considerations of periodicity (Section 2.1), surface variables (Section 2.2), dimensionless quantities (Section 2.3), spectral stability (Section 2.4), and Bloch theory (Section 2.5). In Section 3, we give a detailed description of the Dirichlet–Neumann operator, while in Section 4 we review the linear stability theory. The new "Generalized SCWs" are discussed in Section 5, and we describe our numerical method and results in Sections 6 and 7, respectively.

2. Equations of motion

Our object of study is the motion of the free surface of an ideal (inviscid, irrotational and incompressible) three-dimensional (one vertical and two horizontal directions) deep fluid under the influence of gravity. If the fluid occupies the domain

$$S_\eta := \{(x, y) = (x_1, x_2, y) \in \mathbf{R}^2 \times \mathbf{R} \mid y < \eta(x, t)\}$$

with free surface $\eta = \eta(x, t)$, the well-known equations of motion are [25]

$$\Delta\varphi = 0 \quad \text{in } S_\eta \tag{2.1a}$$

$$\partial_y\varphi \to 0 \quad y \to -\infty \tag{2.1b}$$

$$\partial_t\eta = \partial_y\varphi - \nabla_x\eta \cdot \nabla_x\varphi \quad \text{at } y = \eta \tag{2.1c}$$

$$\partial_t\varphi = -g\eta - \frac{1}{2}\nabla\varphi \cdot \nabla\varphi \quad \text{at } y = \eta, \tag{2.1d}$$

where $\varphi = \varphi(x, y, t)$ is the velocity potential ($\mathbf{u} = \nabla\varphi$) and g is the constant of gravity. These equations are also supplemented with initial conditions

$$\eta(x, 0) = \eta^{(0)}(x), \qquad \varphi(x, \eta(x, 0), 0) = \xi^{(0)}(x),$$

where it suffices (by elliptic theory [26]) to specify φ only at the surface.

2.1. Periodicity

Boundary conditions are also required and, for the study of hexagonal (rectangular) waves that we undertake here, they are periodicity with respect to some lattice

$$\Gamma = \left\{\gamma \in \mathbf{R}^2 \mid \gamma = m_1a_1 + m_2a_2;\, a_1, a_2 \in \mathbf{R}^2;\, m_1, m_2 \in \mathbf{Z}\right\},$$

generated by two linearly independent vectors a_1, a_2. Functions periodic with respect to Γ satisfy

$$\eta(x + \gamma, t) = \eta(x, t), \qquad \varphi(x + \gamma, y, t) = \varphi(x, y, t), \quad \forall\gamma \in \Gamma$$

and this lattice generates the conjugate lattice of wavenumbers

$$\Gamma' := \{k \in \mathbf{R}^2 \mid k \cdot \gamma \in (2\pi)\mathbf{Z}, \forall\gamma \in \Gamma\}$$

so that, e.g., we can express η by its Fourier series

$$\eta(x, t) = \sum_{k\in\Gamma'} \hat{\eta}_k(t)e^{ik\cdot x}. \tag{2.2}$$

Utilizing the notation of Roberts et al. [11,12,27,13] we specialize to "Rectangular" or "Short-Crested Waves" (SCWs) which are periodic both in the direction of propagation and the orthogonal horizontal direction [9,10]. In this work, the periods are set to $L_1 := L_0/\sin(\theta)$ and $L_2 := L_0/\cos(\theta)$ in the parallel and orthogonal directions to propagation, respectively. Roberts used this to describe a L_0-periodic Stokes wavetrain incident upon a vertical wall where θ is the angle between the direction of propagation and the normal to the wall. In this way, $\theta = 0$ corresponds to Stokes waves while $\theta = \pi/2$ represents the case of standing waves. One can also regard this setting as the interaction of two Stokes wavetrains incident upon one another at an angle $\mu = \pi - 2\theta$. If we choose the x_1-axis as the direction of propagation, then the lattice of periodicity is

$$\Gamma = \Gamma_\theta = \left\{\gamma \in \mathbf{R}^2 | \gamma = m_1a_1 + m_2a_2;\right.$$
$$\left. a_1 = \begin{pmatrix} L_0/\sin(\theta) \\ 0 \end{pmatrix}, a_2 = \begin{pmatrix} 0 \\ L_0/\cos(\theta) \end{pmatrix}; m_1, m_2 \in \mathbf{Z}\right\}, \tag{2.3a}$$

and the conjugate lattice is given by

$$\Gamma' = \Gamma'_\theta = \left\{k \in \mathbf{R}^2 \mid k = m_1b_1 + m_2b_2;\right.$$
$$b_1 = \begin{pmatrix} 2\pi\sin(\theta)/L_0 \\ 0 \end{pmatrix}, b_2 = \begin{pmatrix} 0 \\ 2\pi\cos(\theta)/L_0 \end{pmatrix};$$
$$\left. m_1, m_2 \in \mathbf{Z}\right\}. \tag{2.3b}$$

2.2. Surface formulation

Zakharov [28] showed that system (2.1) is, in fact, Hamiltonian in terms of the canonical variables $\eta(x, t)$ and $\xi(x, t) := \varphi(x, \eta(x, t), t)$ with Hamiltonian

$$H_Z = \frac{1}{2}\int_{P(\Gamma)} \left(\int_{-\infty}^{\eta} \nabla\varphi \cdot \nabla\varphi \, dy\right) + g\eta^2 \, dx,$$

where $P(\Gamma)$ is the period cell associated to Γ. A simplification of the formulation and reduction in dimension was realized by

Craig and Sulem [29] with the introduction of the Dirichlet–Neumann operator (DNO) which maps Dirichlet data to Neumann data:

$$G(\eta)[\xi] := \nabla v|_{y=\eta} \cdot N_\eta = \partial_y v|_{y=\eta} - \nabla_x \eta \cdot \nabla_x v|_{y=\eta} \tag{2.4}$$

in reference to the elliptic boundary value problem:

$$\Delta v = 0 \quad \text{in } S_\eta \tag{2.5a}$$

$$\partial_y v \to 0 \quad y \to -\infty \tag{2.5b}$$

$$v(x, \eta(x)) = \xi(x); \tag{2.5c}$$

c.f. (2.1a) and (2.1b). This DNO permits the restatement of H_Z as

$$H_{ZCS} = \frac{1}{2} \int_{P(\Gamma)} \xi\,(G(\eta)\,\xi) + g\eta^2 \, \mathrm{d}x.$$

It can be shown [29,9] that the water wave problem (2.1) can be *equivalently* restated as the following evolution problem

$$\partial_t \eta = G(\eta)[\xi] \tag{2.6a}$$

$$\partial_t \xi = -g\eta - A(\eta) B(\eta, \xi), \tag{2.6b}$$

where

$$A(\eta) := \frac{1}{2\,(1 + \nabla_x \eta \cdot \nabla_x \eta)} \tag{2.7a}$$

$$\begin{aligned} B(\eta, \xi) \;:=\; & \nabla_x \xi \cdot \nabla_x \xi - (G(\eta)[\xi])^2 \\ & - 2\,(G(\eta)[\xi])\,\nabla_x \xi \cdot \nabla_x \eta \\ & + (\nabla_x \xi \cdot \nabla_x \xi)\,(\nabla_x \eta \cdot \nabla_x \eta) - (\nabla_x \xi \cdot \nabla_x \eta)^2 . \end{aligned} \tag{2.7b}$$

Our focus is upon the stability of *traveling* wave solutions of (2.6) and so we move to a reference frame moving uniformly with velocity $c \in \mathbf{R}^2$. In such a frame it is straightforward to show that the governing equations are

$$\partial_t \eta + c \cdot \nabla_x \eta = G(\eta)[\xi] \tag{2.8a}$$

$$\partial_t \xi + c \cdot \nabla_x \xi = -g\eta - A(\eta) B(\eta, \xi). \tag{2.8b}$$

2.3. Dimensionless variables

Before proceeding we mention our (classical) nondimensionalization strategy. We make the scalings

$$x_1 = L x_1', \qquad x_2 = L x_2', \qquad y = L y',$$
$$\eta = a\eta', \qquad \xi = X\xi', \qquad t = T t',$$

with the classical choices [25]

$$X = a\sqrt{Lg}, \qquad T = \sqrt{L/g}, \qquad L = L_0/(2\pi)$$

(recall from Section 2.1 that the traveling wave has wavelengths $L_1 = L_0/\sin(\theta)$ and $L_2 = L_0/\cos(\theta)$ in the x_1 and x_2 directions, respectively). It is not difficult to show that

$$\nabla_x = \frac{1}{L} \nabla_{x'}, \qquad \partial_t = \frac{1}{T} \partial_{t'},$$

while it takes more effort to establish (see Section 3) that

$$G(a\eta') = \frac{1}{L} \sum_{n=0}^{\infty} G_n'(\eta') \alpha^n$$

$$A(a\eta') = \sum_{n=0}^{\infty} A_n'(\eta') \alpha^n$$

$$B(a\eta', X\xi') = \frac{T}{X} \sum_{n=1}^{\infty} B_n'(\eta', \xi') \alpha^n,$$

(in fact $A_{2j+1} = 0$ for $j = 0, 1, \ldots$) where we have defined the slope/steepness parameter

$$\alpha := a/L.$$

A little work shows that (2.8) becomes

$$\partial_{t'} \eta' + c' \cdot \nabla_{x'} \eta' = G_0'[\xi'] + \sum_{n=1}^{\infty} G_n'(\eta')[\xi'] \alpha^n$$

$$\partial_{t'} \xi' + c' \cdot \nabla_{x'} \xi' = -\eta' - \sum_{n=1}^{\infty} \alpha^n \left(\sum_{l=1}^{n} A_{n-l}(\eta') B_l(\eta', \xi') \right),$$

where we have defined the dimensionless velocity

$$c' = \frac{c}{\sqrt{gL}},$$

which, in two dimensions, gives the Froude number. At this point we eliminate the *explicit* dependence upon the (small) dimensionless parameter α by choosing as unknowns the dimensionless quantities

$$\tilde{\eta}(x, t) := \alpha \eta'(x, t) = \frac{\alpha}{a} \eta(x, t) = \frac{1}{L} \eta(x, t),$$

$$\tilde{\xi}(x, t) := \alpha \xi'(x, t) = \frac{\alpha}{X} \xi(x, t) = \frac{1}{\sqrt{L^3 g}} \xi(x, t).$$

Upon dropping primes and tildes, we find the final dimensionless evolution equations in a traveling frame

$$\partial_t \eta + c \cdot \nabla_x \eta = G(\eta)[\xi] \tag{2.9a}$$

$$\partial_t \xi + c \cdot \nabla_x \xi = -\eta - A(\eta) B(\eta, \xi), \tag{2.9b}$$

periodic on the lattice

$$\Gamma_\theta = \left\{ \gamma = \begin{pmatrix} 2\pi m_1 / \sin(\theta) \\ 2\pi m_2 / \cos(\theta) \end{pmatrix} ; \, m_1, m_2 \in \mathbf{Z} \right\},$$

with conjugate lattice

$$\Gamma_\theta' = \left\{ k = \begin{pmatrix} m_1 \sin(\theta) \\ m_2 \cos(\theta) \end{pmatrix} ; \, m_1, m_2 \in \mathbf{Z} \right\};$$

c.f., (2.3a) and (2.3b).

2.4. Spectral stability analysis

Here we briefly recapitulate the spectral stability analysis we have in mind (fully described in [30]). Consider a traveling wave solution of (2.6), i.e., a *steady* solution of (2.9)

$$(\bar{\eta}, \bar{\xi}, \bar{c}) = (\bar{\eta}(x), \bar{\xi}(x), \bar{c}).$$

We seek solutions of the full problem (2.9) in the "spectral stability form"

$$\eta(x, t) = \bar{\eta}(x) + \delta e^{\lambda t} \zeta(x), \qquad \xi(x, t) = \bar{\xi}(x) + \delta e^{\lambda t} \psi(x),$$

where $\delta \ll 1$ measures the perturbation from the steady state, and λ determines the *spectral* stability. Inserting this into (2.9) and using the fact that $(\bar{\eta}, \bar{\xi}, \bar{c})$ are solutions of (2.9), we recover, to order $\mathcal{O}(\delta)$,

$$(\lambda + \bar{c} \cdot \nabla_x) \zeta = G_\eta(\bar{\eta})[\bar{\xi}]\{\zeta\} + G(\bar{\eta})[\psi] \tag{2.10a}$$

$$\begin{aligned} (\lambda + \bar{c} \cdot \nabla_x) \psi \;=\; & -\zeta - A_\eta(\bar{\eta})\{\zeta\} B(\bar{\eta}, \bar{\xi}) \\ & - A(\bar{\eta}) B_\eta(\bar{\eta}, \bar{\xi})\{\zeta\} - A(\bar{\eta}) B_\xi(\bar{\eta}, \bar{\xi})\{\psi\}, \end{aligned} \tag{2.10b}$$

where η and ξ subscripts denote η and ξ variations, respectively. It is not difficult to see that, from (2.7),

$$A_\eta(\bar{\eta})\{\zeta\} = -\frac{\nabla_x \bar{\eta} \cdot \nabla_x \zeta}{(1 + \nabla_x \bar{\eta} \cdot \nabla_x \bar{\eta})^2}$$

$$\begin{aligned} & B_\eta(\bar{\eta}, \bar{\xi})\{\zeta\} \\ & \quad = -2\left(G(\bar{\eta})[\bar{\xi}]\right)\left(G_\eta(\bar{\eta})[\bar{\xi}]\{\zeta\}\right) \\ & \qquad - 2\left(G_\eta(\bar{\eta})[\bar{\xi}]\{\zeta\}\right) \nabla_x \bar{\xi} \cdot \nabla_x \bar{\eta} \end{aligned}$$

$$
\begin{aligned}
&- 2\left(G(\bar\eta)[\bar\xi]\right)\nabla_x\bar\xi\cdot\nabla_x\zeta + 2\left(\nabla_x\bar\xi\cdot\nabla_x\bar\xi\right)\nabla_x\bar\eta\cdot\nabla_x\zeta\\
&- 2\left(\nabla_x\bar\xi\cdot\nabla_x\bar\eta\right)\left(\nabla_x\bar\xi\cdot\nabla_x\zeta\right)\\
B_{\bar\xi}(\bar\eta,\bar\xi)\{\psi\}&\\
&= 2\nabla_x\bar\xi\cdot\nabla_x\psi - 2\left(G(\bar\eta)[\bar\xi]\right)\left(G(\bar\eta)[\psi]\right)\\
&- 2\left(G(\bar\eta)[\psi]\right)\nabla_x\bar\xi\cdot\nabla_x\bar\eta\\
&- 2\left(G(\bar\eta)[\bar\xi]\right)\nabla_x\psi\cdot\nabla_x\bar\eta + 2\left(\nabla_x\bar\xi\cdot\nabla_x\psi\right)\left(\nabla_x\bar\eta\cdot\nabla_x\bar\eta\right)\\
&- 2\left(\nabla_x\bar\xi\cdot\nabla_x\bar\eta\right)\left(\nabla_x\psi\cdot\nabla_x\bar\eta\right),
\end{aligned}
$$

and we defer our discussion of the first variation of the DNO, $G_\eta(\bar\eta)[\bar\xi]\{\zeta\}$, until Section 3.

2.5. Bloch theory

We now write our spectral stability problem (2.10) abstractly as

$$\mathcal{A}(x)\begin{pmatrix}\zeta\\ \psi\end{pmatrix} = \lambda\begin{pmatrix}\zeta\\ \psi\end{pmatrix}. \tag{2.11}$$

The final specification is the boundary conditions that the eigenfunctions (ζ,ψ) must satisfy. For these we use the "Generalized Principle of Reduced Instability" [31] (essentially Floquet Theory, see, e.g., [32]), inspired by the Bloch theory of Schrödinger equations with periodic potentials [33]. This theory allows perturbations

$$(\zeta,\psi)\in H^2_{lu}(\mathbf{R}^2),$$

which are in the Sobolev class of uniformly local L^2 functions. Mielke [31] reduces this study to the "Bloch waves", e.g.,

$$\zeta(x) = e^{ip\cdot x}Z(x),\qquad \psi(x) = e^{ip\cdot x}Y(x),$$

where $Z,Y\in H^2(P(\Gamma))$. As we shall see, it suffices to consider $p\in P(\Gamma')$, the fundamental cell of wavenumbers, and thus (2.11) becomes

$$\mathcal{A}_p(x)\begin{pmatrix}\zeta\\ \psi\end{pmatrix} = \lambda\begin{pmatrix}\zeta\\ \psi\end{pmatrix},$$

where

$$\mathcal{A}_p(x)\begin{pmatrix}\zeta\\ \psi\end{pmatrix} := e^{-ip\cdot x}\mathcal{A}(x)\left[e^{ip\cdot x}\begin{pmatrix}\zeta\\ \psi\end{pmatrix}\right].$$

Mielke's fundamental result is that

$$L^2-\mathrm{spec}(\mathcal{A}) = L^2_{lu}-\mathrm{spec}(\mathcal{A}) = \mathrm{closure}\left(\bigcup_{p\in P(\Gamma')}\mathrm{spec}(\mathcal{A}_p)\right).$$

Thus, we learn about stability with respect to *all* of these perturbations by simply considering $Z,Y\in H^2(P(\Gamma))$ and $p\in P(\Gamma')$. This whole analysis is equivalent to requiring that the functions ζ and ψ satisfy the "Bloch boundary conditions":

$$\zeta(x+\gamma) = e^{ip\cdot\gamma}\zeta(x),\qquad \psi(x+\gamma) = e^{ip\cdot\gamma}\psi(x),\quad \forall\gamma\in\Gamma.$$

Such functions can be expanded in the "generalized" Fourier series

$$\zeta(x) = \sum_{k\in\Gamma'}\hat\zeta_k e^{i(k+p)\cdot x},\qquad \psi(x) = \sum_{k\in\Gamma'}\hat\psi_k e^{i(k+p)\cdot x}; \tag{2.12}$$

c.f. (2.2).

3. The Dirichlet–Neumann operator and its first variation

The one unexplained component of our formulation of the spectral stability problem is the computation of the DNO and its first variation. Many algorithms can be contemplated including finite difference, finite element, finite volume, and integral equation methods. However, we choose the accurate and efficient Method of Operator Expansions (OEs) [34,29,9,35] and provide brief details here (in the case of water of infinite depth). The key observation for the OE methodology is that for sufficiently smooth deformations $\eta = \varepsilon f$, the DNO and its first variation depend *analytically* upon the height/slope parameter $\varepsilon\in\mathbf{R}$ resulting in strongly convergent expansions

$$G(\varepsilon f) = \sum_{n=0}^{\infty}G_n(f)\varepsilon^n,\qquad G_\eta(\varepsilon f) = \sum_{n=0}^{\infty}G_n^{(1)}(f)\varepsilon^n$$

for ε sufficiently small. The OE approach prescribes accurate formulas for the G_n and $G_n^{(1)}$ in terms of Fourier multipliers and convolutions.

In more detail, consider the function

$$v_k(x,y) = e^{ik\cdot x+|k|y},\quad k\in\Gamma'$$

which satisfies (2.5a) and (2.5b) of the elliptic equations governing the definition of the DNO. Inserting this into the definition of the DNO, (2.4), gives

$$G(\varepsilon f)\left[e^{ik\cdot x+|k|\varepsilon f}\right] = \left(|k|-\varepsilon(\partial_x f)(ik)\right)e^{ik\cdot x+|k|\varepsilon f}.$$

Expanding the DNO and exponentials in power series yields

$$
\begin{aligned}
&\left(\sum_{n=0}^{\infty}G_n(f)\varepsilon^n\right)\left[\sum_{m=0}^{\infty}F_m|k|^m\varepsilon^m e^{ik\cdot x}\right]\\
&\quad= \left(|k|-\varepsilon(\partial_x f)(ik)\right)\sum_{n=0}^{\infty}F_n|k|^n\varepsilon^n e^{ik\cdot x},
\end{aligned}\tag{3.1}
$$

where $F_n(x) := f(x)^n/n!$. At order $\mathcal{O}(\varepsilon^0)$ this gives

$$G_0\left[e^{ik\cdot x}\right] = |k|e^{ik\cdot x} = |D|\left[e^{ik\cdot x}\right],$$

which defines the order-one Fourier multiplier $|D|$ in terms of $D = (1/i)\partial_x$. Remarking that any L^2 function ξ can be written in terms of its Fourier series

$$\xi(x) = \sum_{k\in\Gamma'}\hat\xi_k e^{ik\cdot x},$$

we have the action of G_0 on any ξ given by

$$
\begin{aligned}
G_0[\xi] &= G_0\left[\sum_{k\in\Gamma'}\hat\xi_k e^{ik\cdot x}\right]\\
&= \sum_{k\in\Gamma'}\hat\xi_k G_0\left[e^{ik\cdot x}\right] = \sum_{k\in\Gamma'}\hat\xi_k|k|e^{ik\cdot x} =: |D|[\xi].
\end{aligned}\tag{3.2}
$$

At order $n>0$ in (3.1) we find

$$
\begin{aligned}
G_n(f)\left[e^{ik\cdot x}\right] &= F_n|k|^{n+1}e^{ik\cdot x} - (\partial_x f)F_{n-1}(ik)|k|^{n-1}e^{ik\cdot x}\\
&\quad - \sum_{m=0}^{n-1}G_m(f)\left[F_{n-m}|k|^{n-m}e^{ik\cdot x}\right]\\
&= \left(F_n|D|^2 + (Df)F_{n-1}D\right)\left[|D|^{n-1}\left[e^{ik\cdot x}\right]\right]\\
&\quad - \sum_{m=0}^{n-1}G_m(f)\left[F_{n-m}|D|^{n-m}e^{ik\cdot x}\right]\\
&= D\left[F_nD|D|^{n-1}\left[e^{ik\cdot x}\right]\right]\\
&\quad - \sum_{m=0}^{n-1}G_m(f)\left[F_{n-m}|D|^{n-m}\left[e^{ik\cdot x}\right]\right],
\end{aligned}
$$

where we have used $|D|^2 = D^2$ and the product rule for D. Using the Fourier representation of ξ we deduce that

$$G_n(f)[\xi] = D\left[F_n D|D|^{n-1}[\xi]\right] - \sum_{m=0}^{n-1} G_m(f)\left[F_{n-m}|D|^{n-m}[\xi]\right]. \tag{3.3}$$

With these formulas, (3.2) and (3.3), for G_n it is not difficult to formally compute the first variation of the DNO and its perturbation expansion [9,36,37]. For this it is helpful to think of the expansion of the DNO (equivalently) as

$$G(\eta) = \sum_{n=0}^{\infty} G_n(\eta)$$

(G_0 and G_n are given in (3.2) and (3.3), respectively, with f replaced by η). Taking the variation with respect to η we find

$$G_\eta(\eta)\{\zeta\} = \left(\delta_\eta G\right)(\eta)\{\zeta\} = \sum_{n=1}^{\infty}\left(\delta_\eta G_n\right)(\eta)\{\zeta\},$$

where the $n = 0$ term disappears as it is independent of η, and

$$\begin{aligned}&\left(\delta_\eta G_n(\eta)\right)[\xi]\{\zeta\}\\ &= D\left[\zeta\left(\frac{\eta^{n-1}}{(n-1)!}\right)D|D|^{n-1}[\xi]\right]\\ &\quad - \sum_{m=0}^{n-1}\left(\delta_\eta G_m(\eta)\right)\left[\left(\frac{\eta^{n-m}}{(n-m)!}\right)|D|^{n-m}[\xi]\right]\{\zeta\}\\ &\quad - \sum_{m=0}^{n-1} G_m(f)\left[\zeta\left(\frac{\eta^{n-m-1}}{(n-m-1)!}\right)|D|^{n-m}[\xi]\right].\end{aligned}$$

While this formula is absolutely correct, in an expansion in powers of ε, where $\eta = \varepsilon f$, this nth order term is only $\mathcal{O}(\varepsilon^{n-1})$, thus

$$\begin{aligned}G^{(1)}_{n-1}(f)[\xi]\{\zeta\} &= D\left[\zeta F_{n-1} D|D|^{n-1}[\xi]\right]\\ &\quad - \sum_{m=0}^{n-1} G^{(1)}_{m-1}(f)\left[F_{n-m}|D|^{n-m}[\xi]\right]\{\zeta\}\\ &\quad - \sum_{m=0}^{n-1} G_m(f)\left[\zeta F_{n-m-1}|D|^{n-m}[\xi]\right].\end{aligned} \tag{3.4}$$

4. Linear stability theory

To properly frame our discussion of the spectral stability theory of nonlinear traveling water waves we must first discuss the linear theory. The traveling waves we study bifurcate from the trivial state, i.e.

$$(\bar\eta, \bar\xi, \bar c) = (0, 0, c_0),$$

for particular values of the velocity $\bar c = c_0$ which we discuss below, and thus the zeroth order stability result involves the study of these forms in the spectral stability problem (2.10). It is not difficult to see that, in this case, (2.10) becomes

$$\begin{aligned}&(\lambda + c_0\cdot\nabla_x)\zeta_0 = G_0[\psi_0]\\ &(\lambda + c_0\cdot\nabla_x)\psi_0 = -\zeta_0,\end{aligned}$$

or

$$\begin{pmatrix}\lambda_0 + c_0\cdot\nabla_x & -G_0\\ 1 & \lambda_0 + c_0\cdot\nabla_x\end{pmatrix}\begin{pmatrix}\zeta_0\\ \psi_0\end{pmatrix} = 0.$$

Expressing ζ_0 and ψ_0 in terms of their generalized Fourier series

$$\zeta_0(x) = \sum_{k\in\Gamma'}\hat\zeta_{0,k}e^{i(k+p)\cdot x}, \qquad \psi_0(x) = \sum_{k\in\Gamma'}\hat\psi_{0,k}e^{i(k+p)\cdot x},$$

(c.f., (2.12)) this reduces to

$$\begin{pmatrix}\lambda_0 + c_0\cdot(i(k+p)) & -|k+p|\\ 1 & \lambda_0 + c_0\cdot(i(k+p))\end{pmatrix}\begin{pmatrix}\hat\zeta_{0,k}\\ \hat\psi_{0,k}\end{pmatrix} = 0.$$

Given a velocity c_0, and the quasiperiodicity parameter p, we find non-trivial solutions for *all* $k \in \Gamma'$ for *two* choices of the eigenvalue λ_0 which make the determinant function

$$\Lambda(\lambda_0, c_0, k, p) := (\lambda_0 + ic_0\cdot(k+p))^2 + |k+p|$$

equal to zero, i.e.,

$$\begin{aligned}\lambda_0^s(k,p) &= i\left(-c_0\cdot(k+p) + s\sqrt{|k+p|}\right)\\ &= i\left(-c_0\cdot(k+p) + s\sqrt{\omega_{k+p}}\right),\end{aligned} \tag{4.1}$$

where $s = \pm 1$ and $\omega_k := \sqrt{|k|}$ is the dispersion relation. It is important to note that these eigenvalues are *purely imaginary* thus indicating that the trivial, "flat water", state is (weakly) stable. Small perturbations will not grow, but neither will they decay.

The important question, of course, is what happens as we move from trivial (zero-amplitude) traveling waves to non-trivial (finite amplitude) waves. The spectrum will "move" as the wave amplitude, for instance, is varied from zero and the question arises: does one (or more) of the eigenvalues move into the complex right half-plane, i.e., does $\mathrm{Re}\{\lambda^s\} > 0$ for any eigenvalue? The results of MacKay and Saffman [38] (which extend well-known results for *finite dimensional* Hamiltonian systems to the water wave problem) give us a necessary (though not sufficient, see [39]) condition for such an excursion for an eigenvalue. This may only occur *after* "collision" with another eigenvalue. That is, only after an eigenvalue increases its multiplicity larger than one.

Therefore, to detect the "first" instability (i.e., the one for the smallest amplitude traveling wave) it is natural to focus upon eigenvalues of higher multiplicity among the trivial wave spectrum, (4.1). If all eigenvalues are distinct (multiplicity one) for a particular configuration (e.g., a fixed value of $p \in P(\Gamma')$) then there is guaranteed a small "window of stability" for small enough amplitudes [39,30]. However, if one of the eigenvalues has multiplicity two (or higher) there may be "immediate" instability, i.e., instability for *all* amplitudes larger than zero.

The work of Ioualalen and Kharif [17,18] focuses precisely upon these "resonant configurations", i.e., values of $p \in P(\Gamma')$ where eigenvalues of multiplicity two (or higher) exist. These values of p can be characterized by the condition

$$\lambda_0^{s_1}(k_1, p) = \lambda_0^{s_2}(k_2, p), \quad k_1 \neq k_2,$$

and it can be shown that s_2 must be the opposite of s_1. Following McLean's work on the three-dimensional stability of Stokes waves [4,5,40], Ioualalen and Kharif define assorted classes of resonances based upon the parity of the components of the difference $k_1 - k_2$, and then plot the resulting curves in p-space for these classes. For SCW they then indicate, for specified values of the traveling wave amplitude, which values of p give rise to a spectrum with positive real part. While the results are not terribly detailed (they do not give quantitative information on the *magnitude* of the largest real part), they do show that the lowest-order ($k_1 - k_2$ small) resonances are dominant for small amplitudes.

5. Generalized short crested waves

Having discussed the stability of "flat water", we now specialize to the "Generalized Short-Crested Waves" (GSCWs) which are the focus of our investigations here. To begin we will define these GSCWs by recalling the governing equations for water waves in a

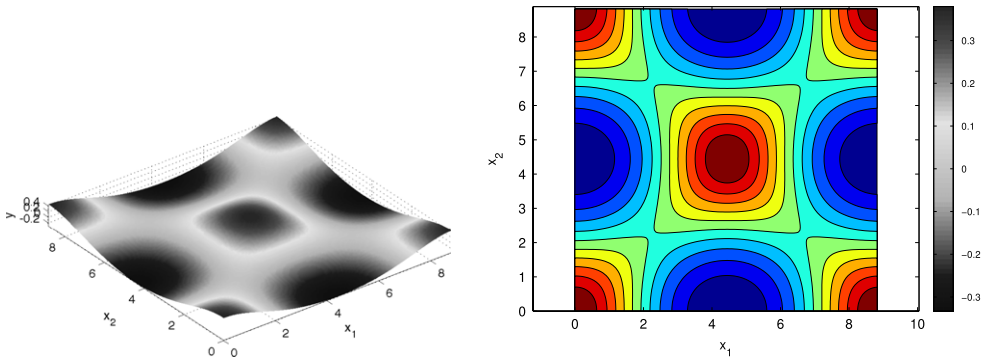

(a) Surface. (a) Contour.

Fig. 1. Plot of a Generalized Short-Crested Wave for $\rho_1/\rho_2 = 1/1$.

reference frame traveling with velocity $\bar{c}$, (2.9), and let us focus on steady, *linear* solutions which satisfy

$$\bar{c}_0 \cdot \nabla_x \bar{\eta}_1 = G_0[\bar{\xi}_1]$$
$$\bar{c}_0 \cdot \nabla_x \bar{\xi}_1 = -\bar{\eta}_1,$$

and, in light of (3.2), become

$$\begin{pmatrix} \bar{c}_0 \cdot \nabla_x & -G_0 \\ 1 & \bar{c}_0 \cdot \nabla_x \end{pmatrix} \begin{pmatrix} \bar{\eta}_1 \\ \bar{\xi}_1 \end{pmatrix} = 0. \tag{5.1}$$

Expanding

$$\bar{\eta}_1(x) = \sum_{k \in \Gamma'} d_k e^{ik\cdot x}, \qquad \bar{\xi}_1(x) = \sum_{k \in \Gamma'} a_k e^{ik\cdot x},$$

we must solve

$$\begin{pmatrix} \bar{c}_0 \cdot (ik) & -|k| \\ 1 & \bar{c}_0 \cdot (ik) \end{pmatrix} \begin{pmatrix} d_k \\ a_k \end{pmatrix} = 0, \tag{5.2}$$

at every wavenumber $k \in \Gamma'$. Non-trivial solutions exist only when a wavenumber k_1 and velocity $\bar{c}_0$ render the matrix on the left hand side singular, i.e. when its determinant is zero

$$0 = -(\bar{c}_0 \cdot k_1)^2 + |k_1| = -(\bar{c}_0 \cdot k_1)^2 + \omega_{k_1}^2.$$

This represents one equation for two unknowns, $\bar{c}_0 \in \mathbf{R}^2$, so we may specify a *second*, linearly independent, wavenumber $k_2 \in \Gamma'$ and demand

$$0 = -(\bar{c}_0 \cdot k_2)^2 + |k_2| = -(\bar{c}_0 \cdot k_2)^2 + \omega_{k_2}^2,$$

resulting (up to a choice of signs) in the linear system

$$\begin{pmatrix} k_1^{(1)} & k_1^{(2)} \\ k_2^{(1)} & k_2^{(2)} \end{pmatrix} \begin{pmatrix} \bar{c}_0^{(1)} \\ \bar{c}_0^{(2)} \end{pmatrix} = \begin{pmatrix} \omega_{k_1} \\ \omega_{k_2} \end{pmatrix}, \qquad k_j = \begin{pmatrix} k_j^{(1)} \\ k_j^{(2)} \end{pmatrix},$$

$$\bar{c}_0 = \begin{pmatrix} \bar{c}_0^{(1)} \\ \bar{c}_0^{(2)} \end{pmatrix}.$$

In this present study, we select $k_1 = (\sin(\theta), \cos(\theta))^T$ and $k_2 = (\sin(\theta), -\cos(\theta))^T$ so that

$$\bar{c}_0 = \begin{pmatrix} 1/\sin(\theta) \\ 0 \end{pmatrix}.$$

With this choice of velocity $\bar{c}_0$ we find solutions to (5.2) at $k = k_1, k_2$ of the form

$$\begin{pmatrix} d_k \\ a_k \end{pmatrix} = A \begin{pmatrix} |k| \\ i\bar{c}_0 \cdot k \end{pmatrix} = A \begin{pmatrix} 1 \\ i \end{pmatrix},$$

together with $d_{-k} = \bar{d}_k$ and $a_{-k} = \bar{a}_k$, for any $A = (\rho/2)e^{i\phi} \in \mathbf{C}$. Thus, we have the quadruply parameterized family of solutions

$$\bar{\eta}_1(x) = \rho_1 \cos(k_1 \cdot x + \phi_1) + \rho_2 \cos(k_2 \cdot x + \phi_2)$$
$$\bar{\xi}_1(x) = -\rho_1 \sin(k_1 \cdot x + \phi_1) - \rho_2 \sin(k_2 \cdot x + \phi_2)$$

for any choices of ρ_j, ϕ_j. We lose no generality by setting $\phi_j = 0$ as this simply sets the maximum for $\bar{\eta}_1$ at the origin, and if we express the amplitudes (ρ_1, ρ_2) in polar coordinates (τ, σ) via

$$\rho_1 = \tau \cos(\sigma), \qquad \rho_2 = \tau \sin(\sigma),$$

then we may set $\tau = 1$ by varying α. However, we are free to vary the "skewness ratio" σ away from $\pi/4$ (the linearization of the classical Short Crested Waves) to any value $-\pi/2 < \sigma < \pi/2$ (note that $\sigma = 0, \pm\pi/2$ constitute Stokes waves in rotated coordinates) which is the linear part of a "Generalized Short Crested Wave" (GSCW).

The procedure we employ for computing the base traveling waves is due to Nicholls and Reitich [15] and is perturbative in nature (see Section 6 for more details). In short this approach is based upon the *strongly convergent* perturbation expansions [41]

$$\bar{c} = \bar{c}(\alpha) = \bar{c}_0 + \sum_{n=1}^{\infty} \bar{c}_n \alpha^n,$$

$$\bar{\eta} = \bar{\eta}(x;\alpha) = \bar{\eta}_1(x) + \sum_{n=2}^{\infty} \bar{\eta}_n \alpha^n,$$

$$\bar{\xi} = \bar{\xi}(x;\alpha) = \bar{\xi}_1(x) + \sum_{n=2}^{\infty} \bar{\xi}_n \alpha^n.$$

The corrections $\{\bar{c}_n\}, n \geq 1$, and $\{\bar{\eta}_n, \bar{\xi}_n\}, n \geq 2$, provide the "nonlinearization" of the traveling profiles, and help further distinguish our GSCWs from the classical SCWs considered by other authors. In Figs. 1–3, we depict surface and contour plots of such traveling waveforms for values of $\cot(\sigma) = \rho_1/\rho_2 = 1/1, 1/2, 1/4$, respectively. We see quite explicitly how asymmetric these waveforms can become despite the symmetry of the underlying geometry ($\theta = 45°$). Fig. 1 shows a classical SCW, while the other forms tend increasingly more towards the Stokes wave with wavenumber $k_2 = (\sin(\theta), -\cos(\theta))^T = \left(1/\sqrt{2}, -1/\sqrt{2}\right)^T$.

6. Numerical method

To complete a numerical simulation of the spectral data $\{\lambda, \zeta(x), \psi(x)\}$ from the stability eigenproblem (2.10) there are many algorithms to be chosen. First, high-fidelity approximations of the traveling wave solutions $\{\bar{c}, \bar{\eta}, \bar{\xi}\}$ must be produced. For this we use the work of Nicholls and Reitich [15] which used the method of Transformed Field Expansions to produce coefficients $\{\tilde{c}_n, \tilde{\eta}_{p,n}, \tilde{u}_{p,l,n}\}$ which generate approximations

$$\bar{c}^N(\alpha) = \sum_{n=0}^{N} \tilde{c}_n \alpha^n,$$

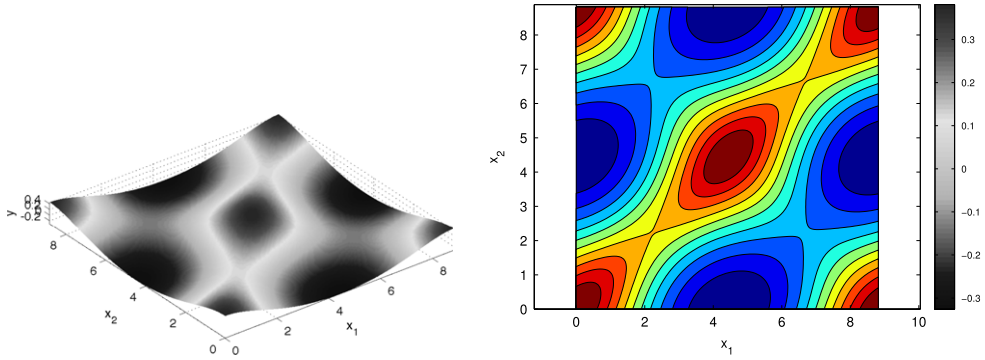

(a) Surface. (a) Contour.

Fig. 2. Plot of a Generalized Short-Crested Wave for $\rho_1/\rho_2 = 1/2$.

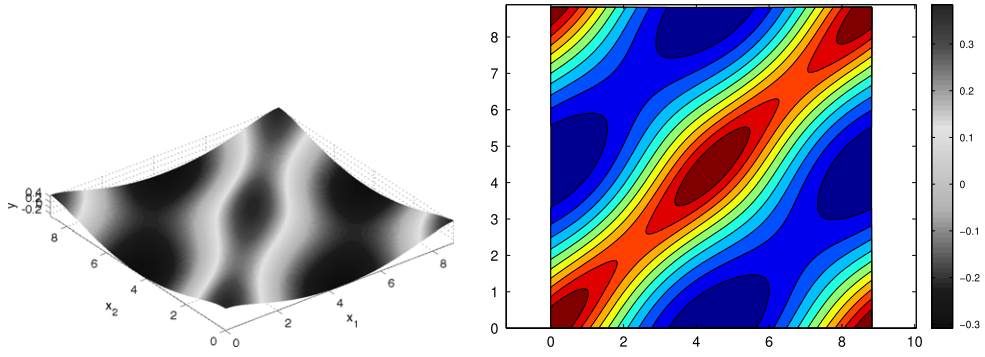

(a) Surface. (a) Contour.

Fig. 3. Plot of a Generalized Short-Crested Wave for $\rho_1/\rho_2 = 1/4$.

$$\bar{\eta}^{N,N_x}(x;\alpha) = \sum_{n=0}^{N} \sum_{|k|<N_x/2} \tilde{\eta}_{n,k} e^{ik\cdot x} \alpha^n,$$

$$\bar{u}^{N,N_x,N_y}(x,y';\alpha) = \sum_{n=0}^{N} \sum_{|k|<N_x/2} \sum_{l=0}^{N_y} \tilde{u}_{n,k,l} e^{ik\cdot x} T_l(y') \alpha^n,$$

where $\bar{u}$ is the *transformed* velocity potential, T_l is the lth Chebyshev polynomial (see [15] for full algorithm details), and $\{N, N_x, N_y\}$ are the perturbation, horizontal, and vertical discretization parameters, respectively. We note that, for our purposes, an approximation to the *surface* velocity potential is more relevant and can be recovered from

$$\bar{\xi}^{N,N_x}(x;\alpha) = \bar{u}^{N,N_x,N_y}(x,0;\alpha),$$

as the transformation maps $y = \eta$ to $y' = 0$.

In addition, we must approximate solutions of the spectral stability problem (2.10). For this we appeal to a Fourier collocation approach and simulate $\zeta(x)$ and $\psi(x)$ with

$$\zeta^{N_x}(x) = \sum_{|k|<N_x/2} \tilde{\zeta}_k e^{i(k+p)\cdot x}, \qquad \psi^{N_x}(x) = \sum_{|k|<N_x/2} \tilde{\psi}_k e^{i(k+p)\cdot x},$$

respectively. These expansions are then inserted into (2.10) and enforced at the equally spaced gridpoints on $P(\Gamma)$. This procedure is straightforward for the forms A, B, A_η, B_η, and B_ξ as derivatives are simulated spectrally, while nonlinearities are evaluated via fast convolutions. The only aspects yet to be addressed are the computation of the DNO, G, and its first variation with respect to η. For this we appeal to the algorithms developed by the author with Fazioli [36,37], which essentially amounts to evaluating the terms G_η and $G_\eta^{(1)}$ from Section 3 via spectral Fourier multipliers and fast convolutions, followed by summation of truncated Taylor series.

Finally, once the matrix representation of the linear operator $\mathcal{A}$ has been formed, we appeal to the LAPACK routine "zgeevx" to find the spectrum for each choice of α. Then, for each value of α, we compute the real part of the eigenvalue with *largest* real part

$$r_{\max}(\alpha) := \max_{p\in P(\Gamma')} \{\mathrm{Re}\{\lambda\} | \lambda \in \mathrm{spec}(\mathcal{A})\}.$$

These are plotted in the next section for fine sampling of α and a certain subset of the $p \in P(\Gamma')$ (in all cases a 10×10 grid), which was determined by the computational resources available to us.

7. Numerical results

We completed extensive numerical simulations for three geometrical configurations:

1. Square Period Cell: $\theta = 45°$,
2. Moderately Skewed Rectangular Period Cell: $\theta = 60°$,
3. Extremely Skewed Rectangular Period Cell: $\theta = 75°$,

and three classes of GSCWs:

1. SCW: $\rho_1/\rho_2 = 1/1$,
2. Moderately Skewed GSCW: $\rho_1/\rho_2 = 1/2$,
3. Extremely Skewed GSCW: $\rho_1/\rho_2 = 1/4$.

For each of these we computed the base traveling waves for a fine sampling of α using the method of Nicholls and Reitich, and then found the quantity $r_{\max}(\theta, \rho_1, \rho_2; \alpha)$ for a 10×10 sampling (equally spaced) of quasiperiods p on the fundamental conjugate period cell $P(\Gamma')$. These quantities indicate the strength of instability for each configuration. To leading order a surface perturbation will grow like

$$Ce^{r_{\max} t}\zeta(x),$$

plus more slowly growing contributions.

We begin with the symmetric geometric configuration $\theta = 45°$ and display in Figs. 4, 6 and 8 plots of $r_{\max}$ versus α for

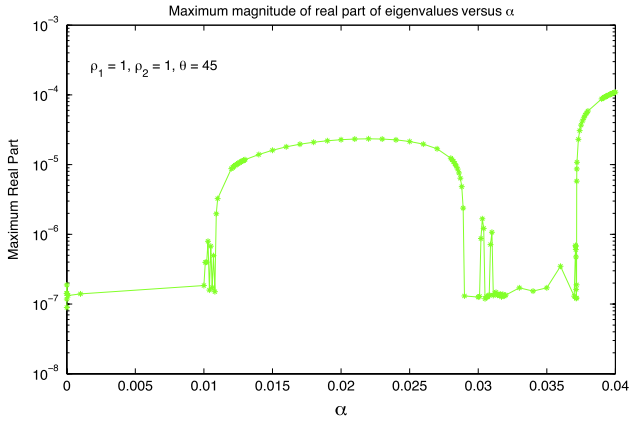

Fig. 4. Plot of maximum real part of an eigenvalue, $r_{\max}$, versus wave height/slope parameter α for $\rho_1/\rho_2 = 1/1, \theta = 45^\circ$.

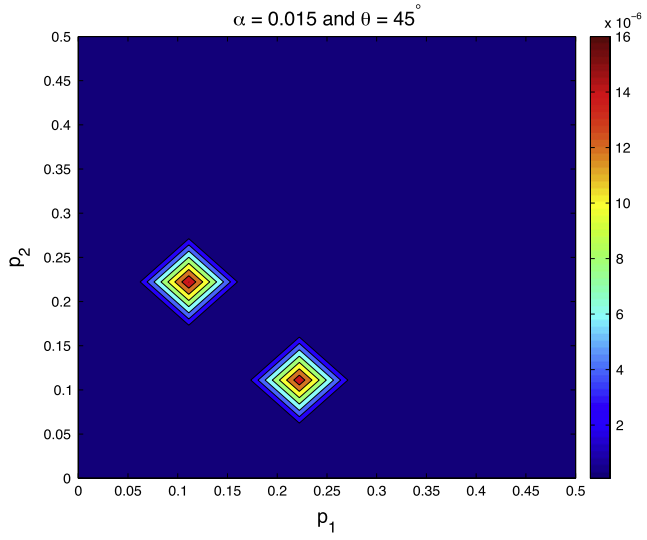

Fig. 5. Plot of maximum real part of an eigenvalue, $r_{\max}$, versus quasiperiod (p_1, p_2) for $\rho_1/\rho_2 = 1/1, \theta = 45^\circ$.

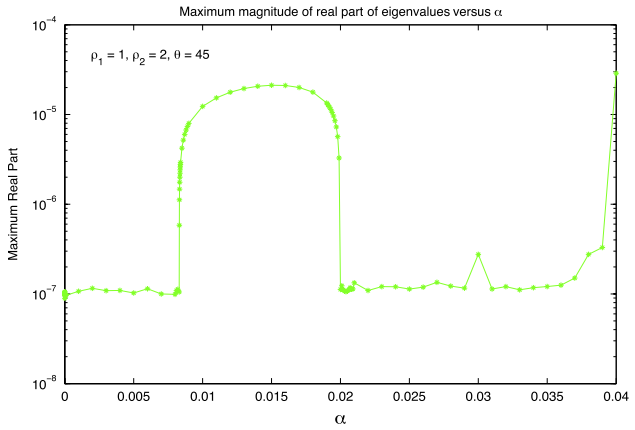

Fig. 6. Plot of maximum real part of an eigenvalue, $r_{\max}$, versus wave height/slope parameter α for $\rho_1/\rho_2 = 1/2, \theta = 45^\circ$.

$\rho_1/\rho_2 = 1/1, 1/2, 1/4$, respectively. For these we notice a few things, first, for the range of quasiperiods p we consider, there is a "Zone of Instability", for each ρ_1/ρ_2 configuration for which waves of smaller *and* larger amplitude are stable (choosing 10^{-7} to be equivalent to zero for our simulations). We see this in the cases $\rho_1/\rho_2 = 1/1$ for $0.01 < \alpha < 0.028$, $\rho_1/\rho_2 = 1/2$ for $0.008 <$

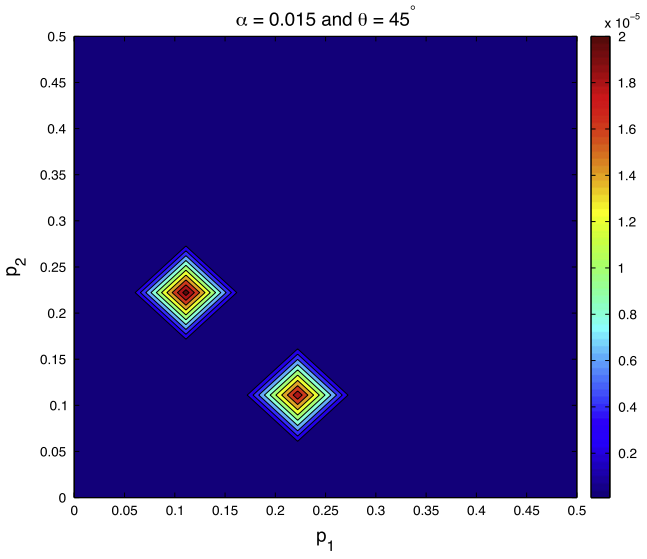

Fig. 7. Plot of maximum real part of an eigenvalue, $r_{\max}$, versus quasiperiod (p_1, p_2) for $\rho_1/\rho_2 = 1/2, \theta = 45^\circ$.

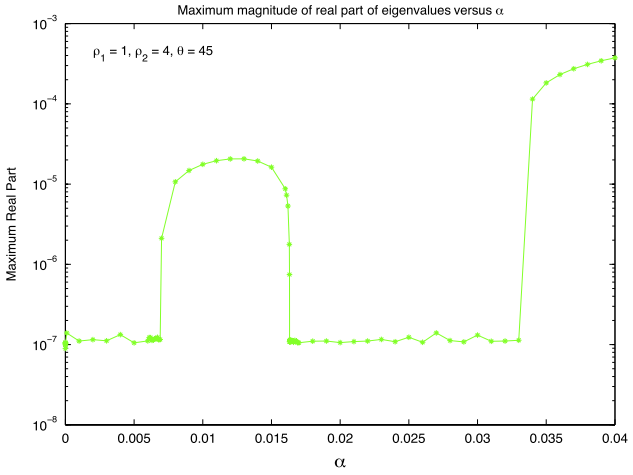

Fig. 8. Plot of maximum real part of an eigenvalue, $r_{\max}$, versus wave height/slope parameter α for $\rho_1/\rho_2 = 1/4, \theta = 45^\circ$.

$\alpha < 0.02$, and $\rho_1/\rho_2 = 1/4$ for $0.006 < \alpha < 0.016$. From these observations we note that, as the ratio ρ_1/ρ_2 is decreased from one, the traveling waves become more unstable in that instability arises for smaller values of α (less nonlinear waves). In Figs. 5, 7 and 9 we display plots of $r_{\max}$ versus the quasiperiod parameter (p_1, p_2) and learn that, in all three cases, the maximum is realized at $(p_1, p_2) = (0.1111, 0.2222)$.

In the mildly asymmetric case $\theta = 60^\circ$ we notice very different stability behavior in Figs. 10, 12 and 14. Here we notice *no* "Zone of Instability", but rather a critical value of α beyond which all larger waves are unstable. This onset of instability happens roughly at $\alpha = 0.015$ for $\rho_1/\rho_2 = 1/1$, $\alpha = 0.013$ for $\rho_1/\rho_2 = 1/2$, and $\alpha = 0.0125$ for $\rho_1/\rho_2 = 1/4$. Again, the waves become more unstable as the ratio ρ_1/ρ_2 decreases. In Figs. 11, 13 and 15 we depict $r_{\max}$ versus the quasiperiod parameter (p_1, p_2) and learn that for the ratios $\rho_1/\rho_2 = 1/1, 1/2$ the maximum is realized at $(p_1, p_2) = (0.05556, 0.5)$, while for the ratio $\rho_1/\rho_2 = 1/4$ it is found at $(p_1, p_2) = (0.05556, 0)$.

Finally, in the strongly asymmetric case $\theta = 75^\circ$ we notice from Figs. 16, 18 and 20 the same behavior as that in the case $\theta = 60^\circ$. Stability for α sufficiently small, followed by instability for all values of α larger than a critical value. This critical behavior happens roughly at $\alpha = 0.012$ for $\rho_1/\rho_2 = 1/1, \alpha = 0.008$

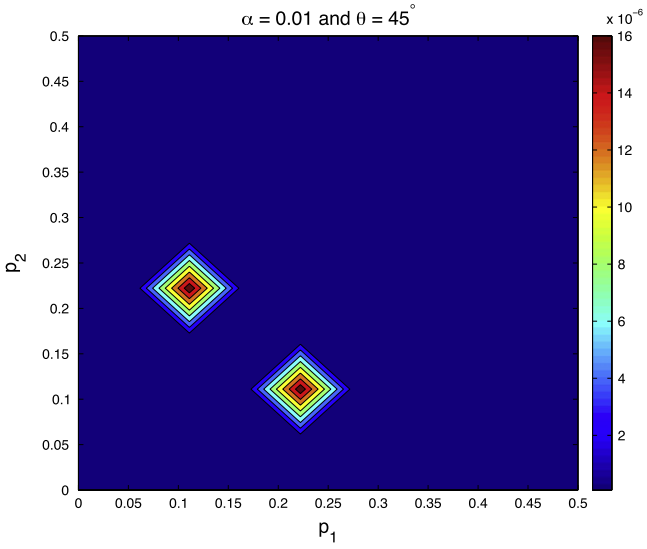

Fig. 9. Plot of maximum real part of an eigenvalue, $r_{\max}$, versus quasiperiod (p_1, p_2) for $\rho_1/\rho_2 = 1/4, \theta = 45°$.

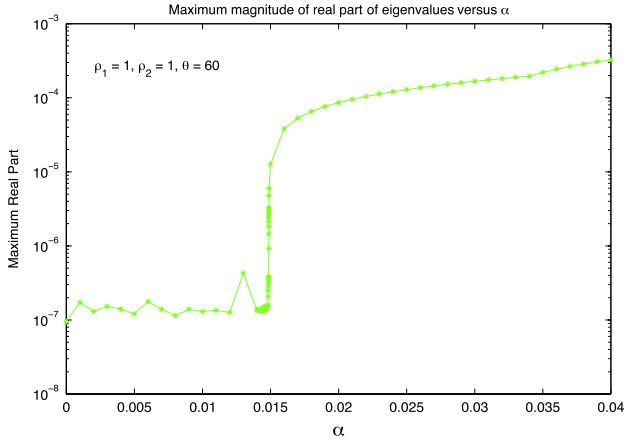

Fig. 10. Plot of maximum real part of an eigenvalue, $r_{\max}$, versus wave height/slope parameter α for $\rho_1/\rho_2 = 1/1, \theta = 60°$.

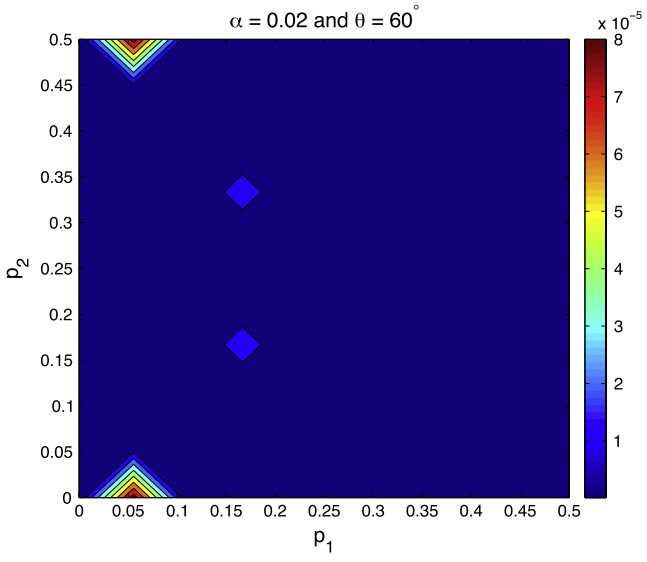

Fig. 11. Plot of maximum real part of an eigenvalue, $r_{\max}$, versus quasiperiod (p_1, p_2) for $\rho_1/\rho_2 = 1/1, \theta = 60°$.

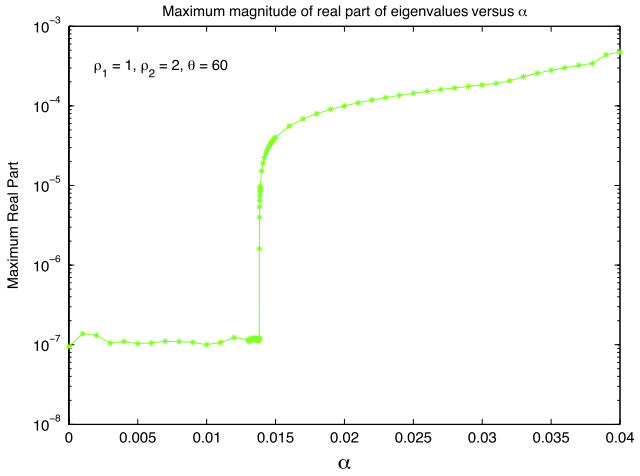

Fig. 12. Plot of maximum real part of an eigenvalue, $r_{\max}$, versus wave height/slope parameter α for $\rho_1/\rho_2 = 1/2, \theta = 60°$.

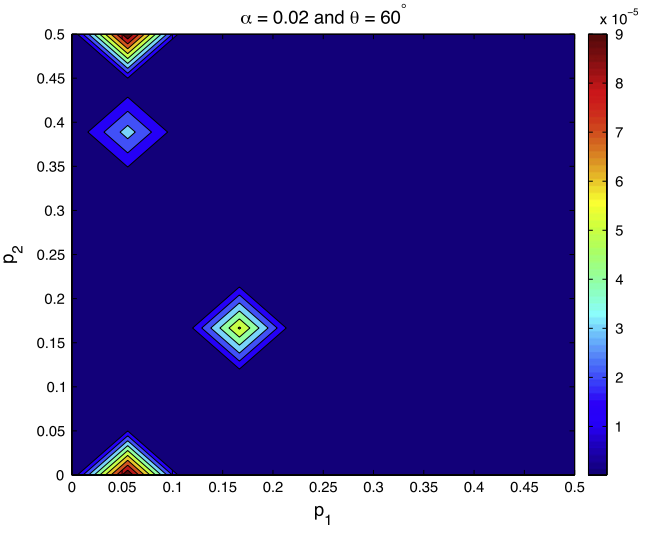

Fig. 13. Plot of maximum real part of an eigenvalue, $r_{\max}$, versus quasiperiod (p_1, p_2) for $\rho_1/\rho_2 = 1/2, \theta = 60°$.

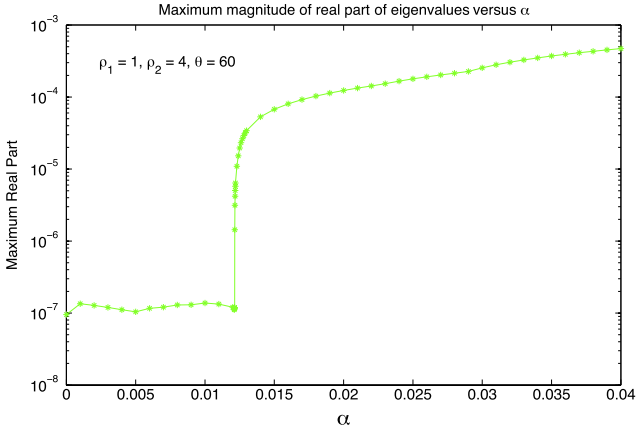

Fig. 14. Plot of maximum real part of an eigenvalue, $r_{\max}$, versus wave height/slope parameter α for $\rho_1/\rho_2 = 1/4, \theta = 60°$.

for $\rho_1/\rho_)$ = 1/2, and α = 0.0075 for ρ_1/ρ_2 = 1/4. Again, there is greater instability for smaller values of ρ_1/ρ_2. From all of these figures we can also deduce a greater degree of instability as the geometric asymmetry parameter is increased away from

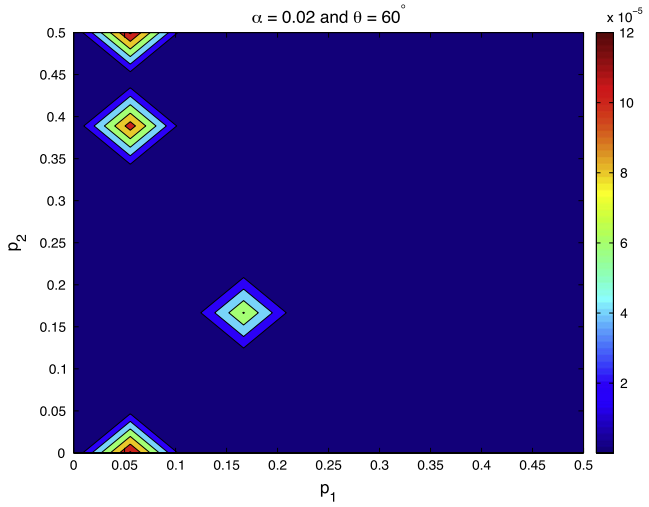

Fig. 15. Plot of maximum real part of an eigenvalue, $r_{\max}$, versus quasiperiod (p_1, p_2) for $\rho_1/\rho_2 = 1/4, \theta = 60°$.

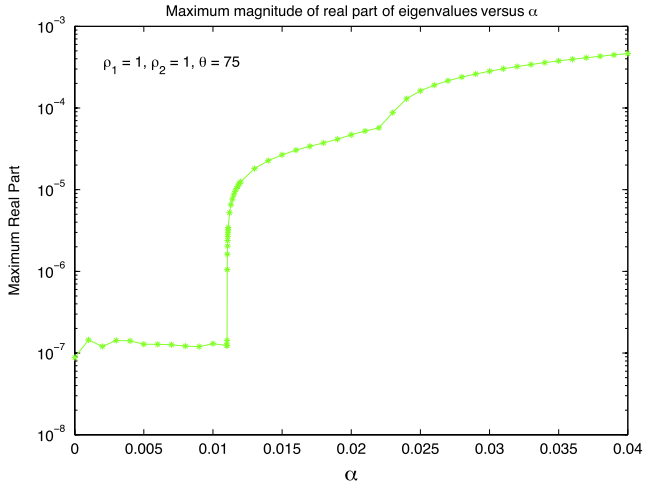

Fig. 16. Plot of maximum real part of an eigenvalue, $r_{\max}$, versus wave height/slope parameter α for $\rho_1/\rho_2 = 1/1, \theta = 75°$.

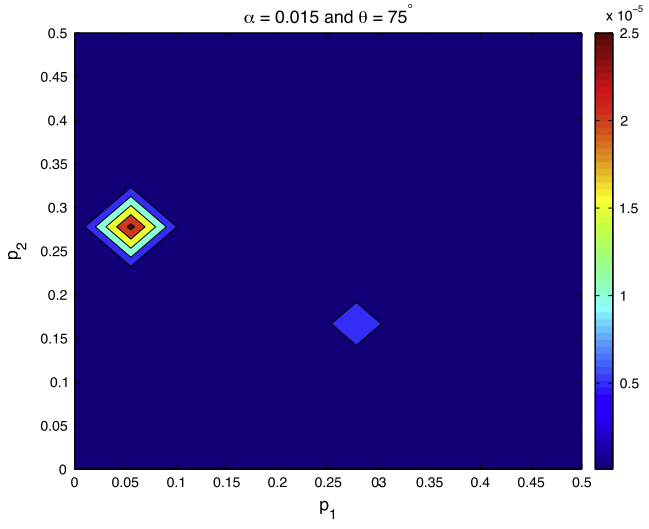

Fig. 17. Plot of maximum real part of an eigenvalue, $r_{\max}$, versus quasiperiod (p_1, p_2) for $\rho_1/\rho_2 = 1/1, \theta = 75°$.

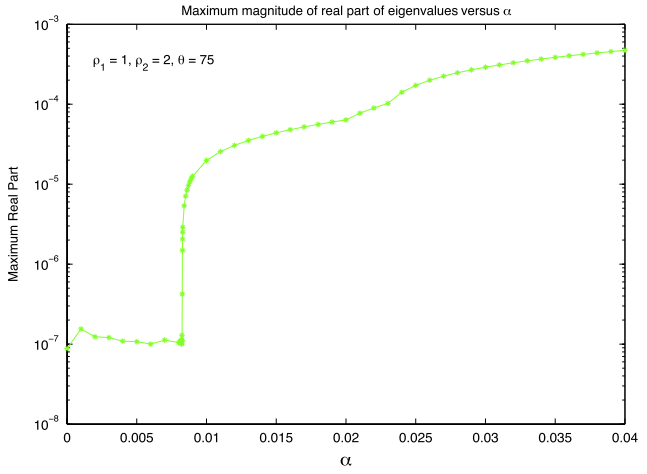

Fig. 18. Plot of maximum real part of an eigenvalue, $r_{\max}$, versus wave height/slope parameter α for $\rho_1/\rho_2 = 1/2, \theta = 75°$.

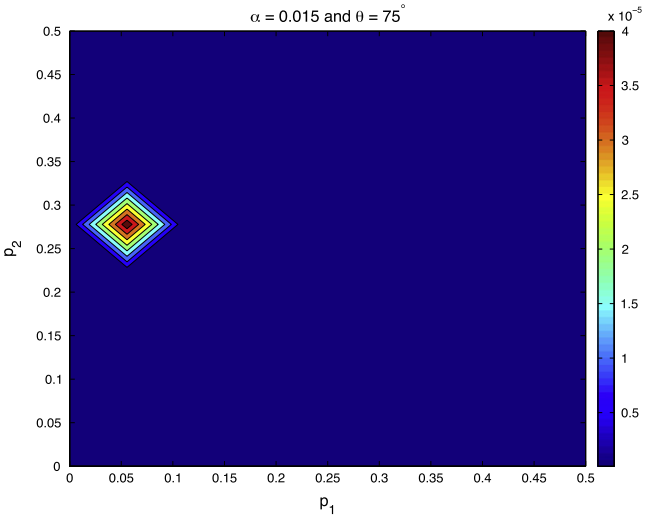

Fig. 19. Plot of maximum real part of an eigenvalue, $r_{\max}$, versus quasiperiod (p_1, p_2) for $\rho_1/\rho_2 = 1/2, \theta = 75°$.

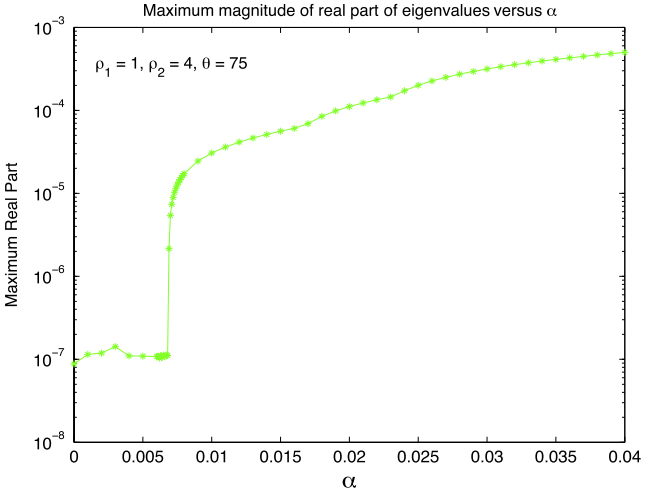

Fig. 20. Plot of maximum real part of an eigenvalue, $r_{\max}$, versus wave height/slope parameter α for $\rho_1/\rho_2 = 1/4, \theta = 75°$.

the symmetric value $\theta = 45°$. In Figs. 17, 19 and 21 we display plots of $r_{\max}$ versus the quasiperiod parameter (p_1, p_2) and learn that, in all three cases, the maximum is realized at $(p_1, p_2) = (0.05556, 0.2778)$.

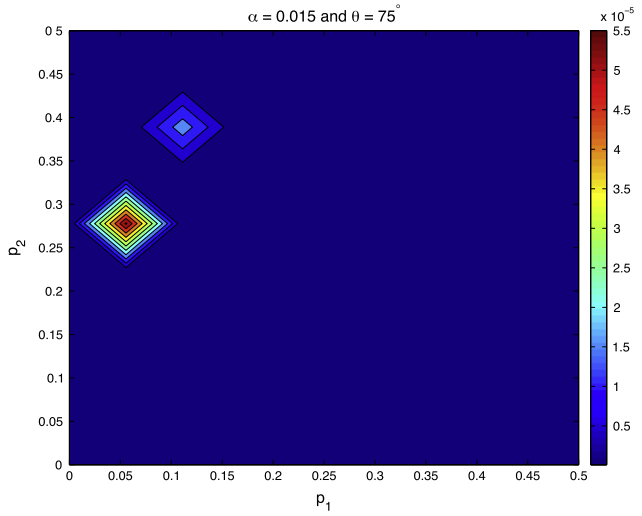

Fig. 21. Plot of maximum real part of an eigenvalue, $r_{\max}$, versus quasiperiod (p_1, p_2) for $\rho_1/\rho_2 = 1/4, \theta = 75^\circ$.

Acknowledgments

TM gratefully acknowledges support from the Department of Energy as a graduate fellow under Award No. DE-SC0001549.

DPN gratefully acknowledges support from the National Science Foundation through grants Nos. DMS-0810958 and DMS-1115333, and the Department of Energy under Award No. DE-SC0001549.

References

[1] T.B. Benjamin, J.E. Feir, The disintegration of wave trains on deep water. part I. theory, J. Fluid Mech. 27 (1967) 417–430.
[2] M.S. Longuet-Higgins, The instabilities of gravity waves of finite amplitude in deep water. I. superharmonics, Proc. R. Soc. Lond. Ser. A 360 (1703) (1978) 471–488.
[3] M.S. Longuet-Higgins, The instabilities of gravity waves of finite amplitude in deep water. II. subharmonics, Proc. R. Soc. Lond. Ser. A 360 (1703) (1978) 489–505.
[4] J.W. McLean, Y.C. Ma, D.U. Martin, P.G. Saffman, H.C. Yuen, Three–dimensional instability of finite–amplitude water waves, Phys. Rev. Lett. 46 (13) (1981) 817–820.
[5] John W. McLean, Instabilities of finite-amplitude water waves, J. Fluid Mech. 114 (1982) 315–330.
[6] C. Kharif, A comparison between 3 and 2 dimensional instabilities of very steep gravity-waves, J. Mech. Theor. Appl. 6 (6) (1987) 843–864.
[7] C. Kharif, A. Ramamonjiarisoa, Deep-water gravity-wave instabilities at large steepness, Phys. Fluids 31 (5) (1988) 1286–1288.
[8] Frédéric Dias, Christian Kharif, Nonlinear gravity and capillary-gravity waves, in: Annual Review of Fluid Mechanics, Vol. 31, Annual Reviews, Palo Alto, CA, 1999, pp. 301–346.
[9] David P. Nicholls, Traveling water waves: Spectral continuation methods with parallel implementation, J. Comput. Phys. 143 (1) (1998) 224–240.
[10] Walter Craig, David P. Nicholls, Traveling gravity water waves in two and three dimensions, Eur. J. Mech. B Fluids 21 (6) (2002) 615–641.
[11] A.J. Roberts, Highly nonlinear short-crested water waves, J. Fluid Mech. 135 (1983) 301–321.
[12] A.J. Roberts, D.H. Peregrine, Notes on long-crested water waves, J. Fluid Mech. 135 (1983) 323–335.
[13] T.R. Marchant, A.J. Roberts, Properties of short-crested waves in water of finite depth, J. Aust. Math. Soc. Ser. B 29 (1) (1987) 103–125.
[14] Walter Craig, David P. Nicholls, Traveling two and three dimensional capillary gravity water waves, SIAM J. Math. Anal. 32 (2) (2000) 323–359.
[15] David P. Nicholls, Fernando Reitich, Rapid, stable, high-order computation of traveling water waves in three dimensions, Eur. J. Mech. B Fluids 25 (4) (2006) 406–424.
[16] David P. Nicholls, Fernando Reitich, On analyticity of traveling water waves, Proc. R. Soc. Lond., A 461 (2057) (2005) 1283–1309.
[17] M. Ioualalen, C. Kharif, Stability of three-dimensional progressive gravity waves on deep water to superharmonic disturbances, Eur. J. Mech. B Fluids 12 (3) (1993) 401–414.
[18] Mansour Ioualalen, Christian Kharif, On the subharmonic instabilities of steady three-dimensional deep water waves, J. Fluid Mech. 262 (1994) 265–291.
[19] Sergei I. Badulin, Victor I. Shrira, Christian Kharif, Mansour Ioualalen, On two approaches to the problem of instability of short-crested water waves, J. Fluid Mech. 303 (1995) 297–326.
[20] Olivier Kimmoun, Mansour Ioualalen, Christian Kharif, Instabilities of steep short-crested surface waves in deep water, Phys. Fluids 11 (6) (1999) 1679–1681.
[21] M. Ioualalen, A.J. Roberts, C. Kharif, On the observability of finite-depth short-crested water waves, J. Fluid Mech. 322 (1996) 1–19.
[22] Mansour Ioualalen, Christian Kharif, Anthony Roberts, Stability regimes of finite depth short–crested water waves, J. Phys. Oceanogr. 29 (9) (1999) 2318–2331.
[23] Mansour Ioualalen, Makoto Okamura, Structure of the instability associated with harmonic resonance of short-crested waves, J. Phys. Oceanogr. 32 (5) (2002) 1331–1337.
[24] Marc Francius, Christian Kharif, Three-dimensional instabilities of periodic gravity waves in shallow water, J. Fluid Mech. 561 (2006) 417–437.
[25] Horace Lamb, Hydrodynamics, sixth ed., Cambridge University Press, Cambridge, 1993.
[26] Lawrence C. Evans, Partial Differential Equations, American Mathematical Society, Providence, RI, 1998.
[27] A.J. Roberts, L.W. Schwartz, The calculation of nonlinear short-crested gravity waves, Phys. Fluids 26 (1983) 2388–2392.
[28] Vladimir Zakharov, Stability of periodic waves of finite amplitude on the surface of a deep fluid, J. Appl. Mech. Tech. Phys. 9 (1968) 190–194.
[29] Walter Craig, Catherine Sulem, Numerical simulation of gravity waves, J. Chem. Phys. 108 (1993) 73–83.
[30] David P. Nicholls, Spectral stability of traveling water waves: eigenvalue collision, singularities, and direct numerical simulation, Physica D 240 (4–5) (2011) 376–381.
[31] Alexander Mielke, Instability and stability of rolls in the Swift–Hohenberg equation, Comm. Math. Phys. 189 (3) (1997) 829–853.
[32] Bernard Deconinck, J. Nathan Kutz, Computing spectra of linear operators using the Floquet–Fourier–Hill method, J. Comput. Phys. 219 (1) (2006) 296–321.
[33] Michael Reed, Barry Simon, Methods of Modern Mathematical Physics. IV. Analysis of Operators, Academic Press [Harcourt Brace Jovanovich Publishers], New York, 1978.
[34] D. Michael Milder, An improved formalism for rough-surface scattering of acoustic and electromagnetic waves, in: Proceedings of SPIE — The International Society for Optical Engineering (San Diego, 1991), vol. 1558, Int. Soc. for Optical Engineering, Bellingham, WA, 1991, pp. 213–221.
[35] David P. Nicholls, Fernando Reitich, Analytic continuation of Dirichlet–Neumann operators, Numer. Math. 94 (1) (2003) 107–146.
[36] C. Fazioli, David P. Nicholls, Parametric analyticity of functional variations of Dirichlet–Neumann operators, Differential Integral Equations 21 (5–6) (2008) 541–574.
[37] Carlo Fazioli, David P. Nicholls, Stable computation of variations of Dirichlet–Neumann operators, J. Chem. Phys. 229 (3) (2010) 906–920.
[38] R.S. MacKay, P.G. Saffman, Stability of water waves, Proc. R. Soc. Lond. A 406 (1986) 115–125.
[39] David P. Nicholls, Spectral data for traveling water waves: singularities and stability, J. Fluid Mech. 624 (2009) 339–360.
[40] John W. McLean, Instabilities of finite-amplitude gravity waves on water of finite depth, J. Fluid Mech. 114 (1982) 331–341.
[41] David P. Nicholls, Fernando Reitich, Shape deformations in rough surface scattering: cancellations, conditioning, and convergence, J. Opt. Soc. Amer. A 21 (4) (2004) 590–605.